Electronic Supplementary Information:

TiN nanopillar-enhanced laser desorption and ionization of various analytes

Yuri Yamada, * *Kenichi Yatsugi, Masakazu Murase, and Norihiro Mizoshita* *

Toyota Central Research & Development Labs., Inc. 41-1 Yokomichi, Nagakute, Aichi 480-1192, Japan.

*Corresponding authors: Yuri Yamada (e4610@mosk.tytlabs.co.jp)
Norihiro Mizoshita (nmizoshita@mosk.tytlabs.co.jp)

<Table of Contents>

<S1> Additional experimental details.

Preparation of TiN nanopillar arrays and the TiN thin film.

The electron beam (EB) deposition was conducted in the oblique angle configuration to yield the Ti nanopillar arrays. Silicon substrates were placed on a rotatable table, which was set at a parallel distance of 40 mm and a vertical height of 250 mm from a granular Ti metal (99.9%, Kojundo Chemical Lab., Saitama, Japan) in a carbon crucible. The EB deposition was operated using L-045E electron-beam deposition system (Canon Anelva, Kanagawa, Japan) with a gas pressure of less than 1.0×10^{-3} Pa, and a deposition rate of 2 Å/s. The substrate was rotated at 4.6 rpm and the deposition was maintained until the Ti pillar grew about 300-350 nm. The obtained Ti nanopillar was annealed at 800 °C for 1 h under ammonia atmosphere, yielding TiN nanopillars (denoted as TiN-p). The flow rates of the ammonia and argon are maintained at 500 ml/min, and 100 ml/min, respectively. For some samples, thin TiN film was deposited on silicon substrate prior to the TiN pillar fabrication, which did not influence significantly on the performance of LDI-MS. To investigate the morphological effect on LDI-MS, TiN film (without nanopillar, denoted as TiN-f) was fabricated. The identical EB deposition parameters as for TiN nanopillars were used under normal angle configuration (vertical deposition), followed by annealing under ammonia atmosphere. For the electromagnetic simulation, the intrinsic values of thermal and optical properties of TiN are necessary. And ideally, the optical properties are required to be measured on an optically flat surface (model surface). As an optical model substrate, TiN thin film was fabricated using RF sputtering method. This process was performed under an Ar and N_2 gas mixture using Ti metal as a sputtering target. The thin TiN film with the thickness of 100 nm was deposited on Si substrate.

Characterizations.

A Shimadzu UV-3600 spectrometer (Kyoto, Japan) was used to measure specular reflection spectra of the TiN substrates at a 5° angle of incidence. The crystal structure was characterized by X ray diffraction (XRD) measurements on a Rigaku Ultima IV diffractometer (Tokyo, Japan) with CuKα radiation at an accelerating voltage of 40 kV. The surface and cross-sectional images of the obtained films were recorded on a Hitachi S-4800 field emission scanning electron microscope (FE-SEM, Tokyo, Japan).

LDI-MS using TiN substrate.

TiN nanopillar substrate was attached onto an ITO (indium tin oxide) coated slide glass with a double-sided conductive carbon tape and then inserted into the instrument using the exclusive adjuster. Careful attention was paid to adjust the height of the sample surface to that of the target plate. Individual conditions, including measurement mode and composition of solvent, depending on target molecules are tabulated in Table S1. To facilitate ionization and signal detection, citric acid (0.02 μmol/μL) was further added. For the detection of IgG, diammonium hydrogen citrate solution (0.02 μmol/μL) was added in replacement of citric acid. A 0.5–1.0 μL aliquot of the analyte solution was spotted onto the substrate surface and then allowed to dry at ambient temperature. MS spectra were acquired automatically at 1–1.5 square millimeter area with a raster width of 100 μm in a random walk laser mode. A total of 20–100 individual laser shots were accumulated at each spot with a laser power of 40–90%, depending on optimization of spectra for each sample. The obtained mass spectra were analyzed with flexImaging 4.1 software and the averaged spectrum at each spot was acquired. The *m/z* values were manually chosen, and two-dimensional ion density maps were generated. Unless otherwise noted, the average mass spectra selected from one spot are exhibited. The signal-to-noise (*S/N*) ratios were determined from the accumulated spectra automatically using the flexAnalysis 3.4 software. For comparison purpose, the same methods of substrate setting and analytical sample preparations as those for TiN-p were employed for the measurements using TiN-f and TiN nanoparticles. A solution of TiN nanoparticles (20 mg/mL) was prepared by dispersing them in a mixture of ACN and 0.1 vol% TFA (3/7, v/v), followed by sonication for 0.5 h. The particle solution (1.0 μL) was pipetted onto a silicon substrate and dried at ambient temperature.

Table S1 Target molecules and the conditions for the LDI measurements

Target molecule	Average molecular weight	Mode	0.1%TFA:ACN (v:v)
Adenosin	267.2	Reflectron	50:50
Verapamil	454.6	Reflectron	100:0
Dipalmitoylphosphatidylcholine (DpPC)	734	Reflectron	100:0
β-cyclodextrin (β-CD)	1135	Reflectron	70:30
Maltoheptaose	1153	Reflectron	100:0
Angiotensin 1 (A1)	1296	Reflectron	100:0
Polyethylene glycol 4000 (PEG4000)	3000	linear	70:30
Amyloid β-Protein (Human, 1-40) (Amyloid β)	4329.8	linear	30:70
Insulin	5807	linear	100/0
Ubiquitin	8560	linear	70:30
Cytochrome C	12327	linear	80:20
Myoglobin	17800	linear	50:50
Trypsinogen	24000	linear	50:50
Bovine serum albumin (BSA)	66000	linear	100:0
Transferrin	79800	linear	100:0
Immunoglobulin G (IgG)	149000	linear	100:0

MALDI-Time of Flight (TOF) MS.

CHCA was dissolved in a mixture of ACN and 0.1 vol% TFA (3/7, v/v). The solution was vortexed and then centrifuged, leaving a clear saturated matrix solution. The matrix solution and the stock solutions of analyte were mixed (1/1, v/v), and a 1.0 μL of mixture was applied to a standard steel MALDI target plate, followed by drying at room temperature. Identical measurement conditions, such as laser power, number of shots, and sample concentration, were employed in MALDI-TOF MSI and TiN-MSI.

<S2> Electromagnetic and heat-transfer simulation details.

The simulation models and the FEM mesh used in this study are show in Figure S1. The simulation models consist of the SiO_2 layer, the TiN pillar (layer), and the vacuum space acting as a finite boundary condition (Figure S1A1, B1). The SiO_2 layer was incorporated as an optically non-absorbing layer. Several SEM images were taken and dimensions of 50 pillars were measured using a commercial software "Image J" to evaluate a diameter, a height, and a pitch of TiN pillars. The averaged values of 60 nm, 300 nm, and 93 nm were determined, respectively. The thickness of TiN layers (350 nm) was determined directly from a side view SEM image. A triangular mesh unit was applied, where the maximum mesh sizes of 23.7 was used for the TiN layers and 59.2 for the SiO_2 and the vacuum layers, respectively. These values correspond to 1/15, and 1/6 of the irradiated laser wavelength (355 nm). Please note that TiN-p has structural distribution and shallow roughness was formed on the surface of TiN-f (Figure S4), but the cylindrical pillars and flat surface were employed as the simulation models for TiN-p and TiN-f respectively to simplify the simulation. The same model used for TiN-p was used to simulate Si nanopillar substrate.

Firstly, we conducted the electromagnetic field simulation and then, proceeded to the heat transfer simulation. The electromagnetic wave was irradiated along the normal (z axis) to the film surface, which was regarded as the laser shot of 355 nm during the LDI measurement. The power of the electromagnetic wave was set as 1.0×10^{-8} W/nm^2.[1] In the heat transfer simulation, the irradiation time was set as 5 ns to fit the duration of the laser pulse used in the LDI-MS measurements. The heat generation upon the laser irradiation was simulated where the initial temperature of the film surface was set as 293 K. Only one pulse was applied, and the propagation of the irradiated laser energy was calculated. Table S2 summarizes the parameters of TiN and Si used in the simulation.

The optical parameters of TiN were measured on the TiN sputtered film. The refractive index (*n*) and the extinction coefficient (*k*) were determined by spectroscopic ellipsometry measurements of TiN sputtered film using an M-2000U (J A Woollam Co., Inc.).[2] Relative amplitude ratio Ψ and phase difference Δ between s- and p- polarizations were measured with incident angles of 55°,60°, and 65°, respectively. An optical model was fitted to the measured values to determine the complex refractive index (*n* - *ik*). The values for the thermal conductivity, the density, and the specific heat were taken from the references. Figure S2 shows reflectance and transmittance spectra of TiN sputtered film.

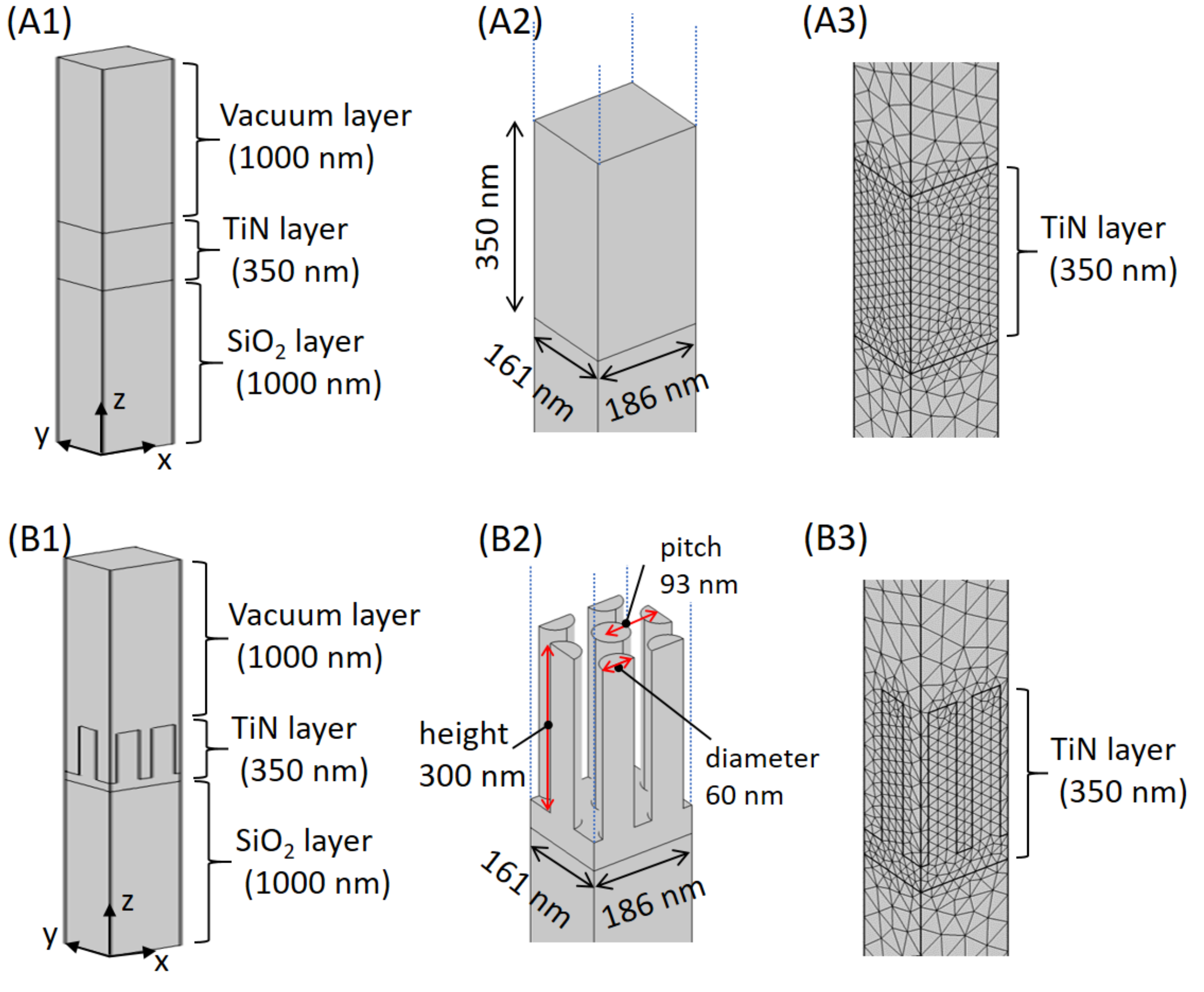

Fig. S1 Dimensions of computational domain for (A1) TiN film and (B1) TiN pillar arrays. (A2) and (B2) are the magnified images of TiN layers depicted in (A1), and (B1), respectively. Surface mesh for (A3) TiN film and (B3) TiN pillar arrays. The same model and mesh of TiN pillar arrays were used to simulate the heat transfer of Si pillar arrays.

Table S2 Physical parameters used for simulations.

Property	Value		Unit
	TiN	Si	
Refractive index (*n*)	2.18[a]	5.61[c]	
Extinction coefficient (*k*)	1.06[a]	3.03[c]	
Thermal conductivity (κ)	16.72[b]	160[d]	W/m×K
Density (d)	5430[b]	2329	kg/m^3
Specific heat (C_p)	522.5[b]	700[e]	J/kg×K

a: Measured values on spectroscopic ellipsometry.

b-e: Taken from Ref 3–6.

<References>

1. Dreisewerd, K.; Schürenberg, M.; Karas, M.; Hillenkamp, F. *Int. J. Mass Spectrom. Ion Processes*, **1995**, 141.127‑148.

2. Yamada, Y.; Ito, K.; Miura, A.; Harada, M.; Matsunaga, T.; Kato, Y.; Matsui, T.; Wakayama, H. *Eur. Polym. J*, **2018**, 107, 96‑104.

3. Choi, S. G.; Ha, T-J.; Yu, B-G.; Shin, S.; Cho, H. H.; Park, H-H. *Thin Solid Films* **2007**, 516, 212‑215.

4. Aspnes, D. E.; Studna. A. A. *Phys. Rev. B* **1983**, 27, 985-1009.

5. Glassbrenner, C. J.; Slack, G. A. *Phys. Rev.* **1964**, *134*, A1058–A1069.

6. Wang, R-j.; Wang, J-w.; Lijin, B-q.; Zhu, Z-f. *Appl. Therm. Eng.***2018***,* 133, 428-438.

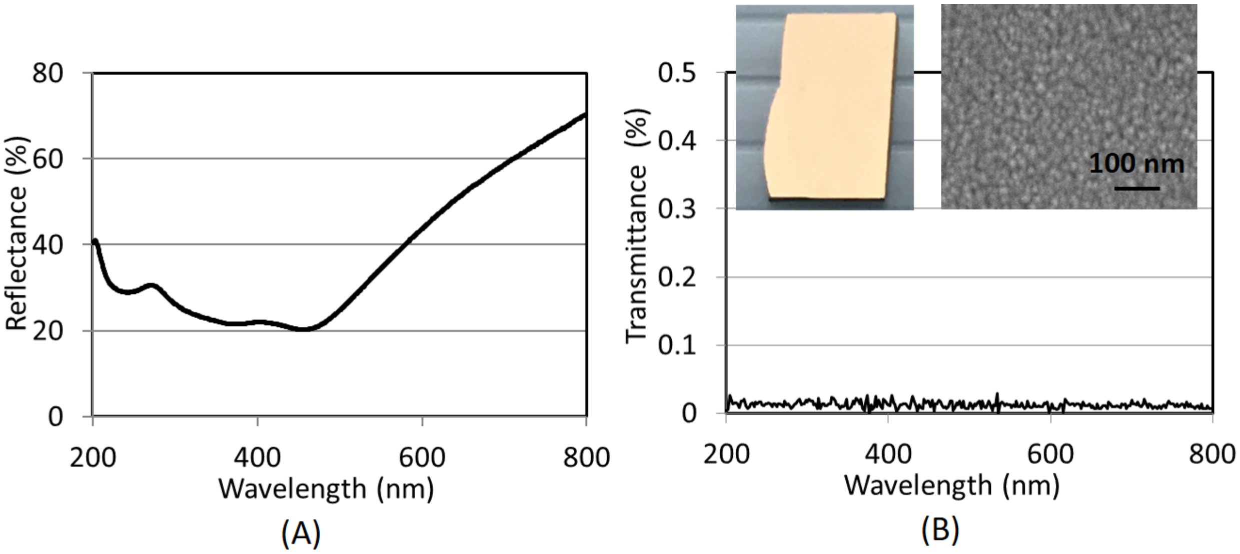

Fig. S2 Optical measurements of TiN sputtered film. (A) Reflectance and (B) transmittance spectra. The transmittance spectrum was collected against the quartz substrate with a Shimadzu UV-3600 spectrometer. Insets in (B) are a photographic image and a top-view SEM image. A reflective metallic color is confirmed on TiN film.

<S3> X-ray photoelectron spectroscopy (XPS).

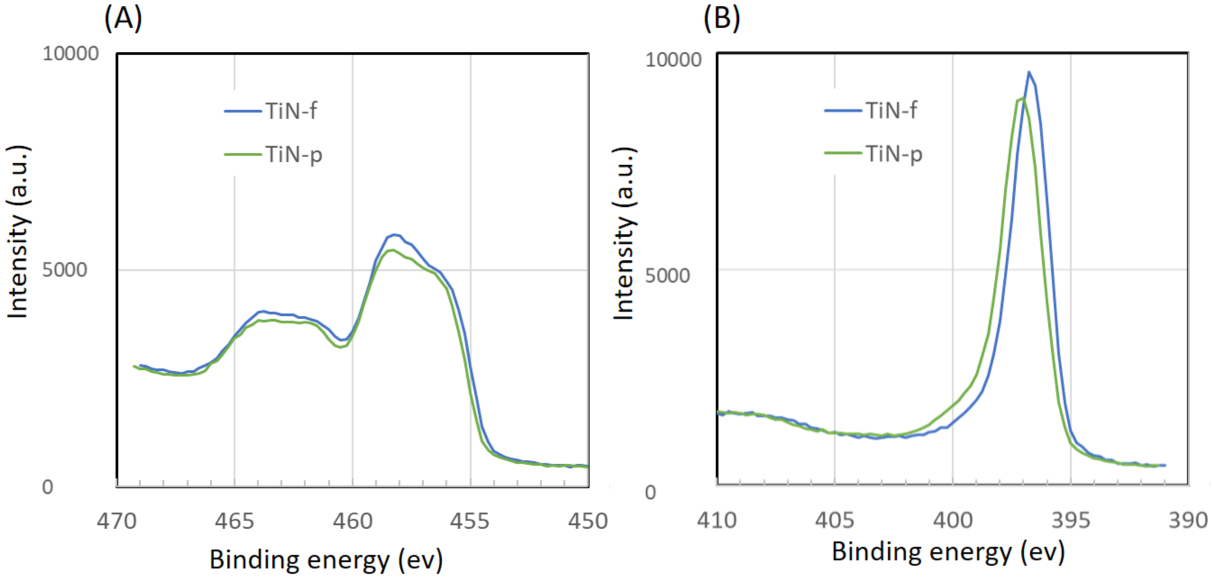

Fig. S3 XPS spectra of the TiN-f and TiN-p. The narrow-scan spectra of (A) the Ti2p and (B) the N1s regions. The measurements were conducted using a Quantera SXM (ULVAC-PHI, Inc.) with monochromated Al Kα radiation at a take-off angle of 45°. The existence of N atom on the surface is confirmed.

<S4> Photographic images of TiN substrates.

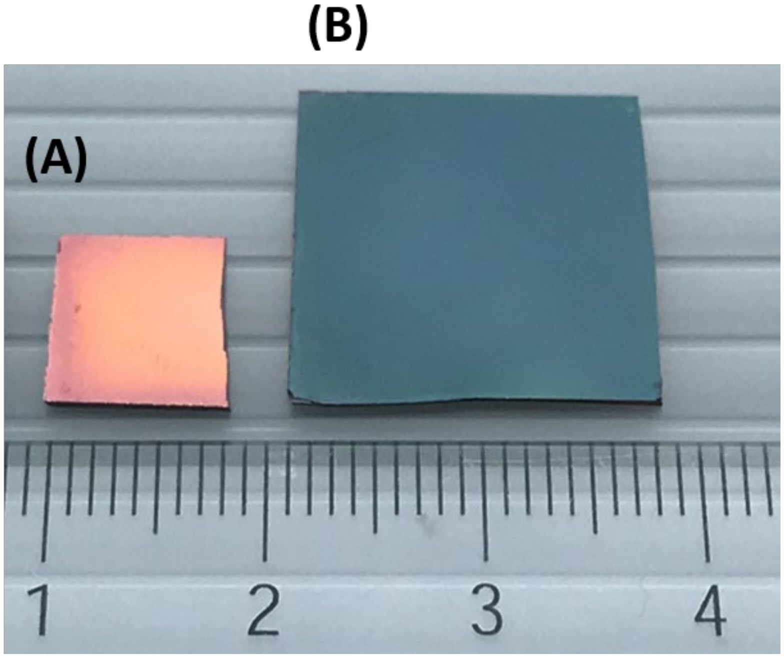

Fig. S4 Photographic images of (A) TiN-f, and (B) TiN-p under natural light. The extinction of reflective metallic color and uniformly dark color of (B) indicates that TiN nanopillars were successfully fabricated at centimeter scale.

<S5> SEM images of TiN-f.

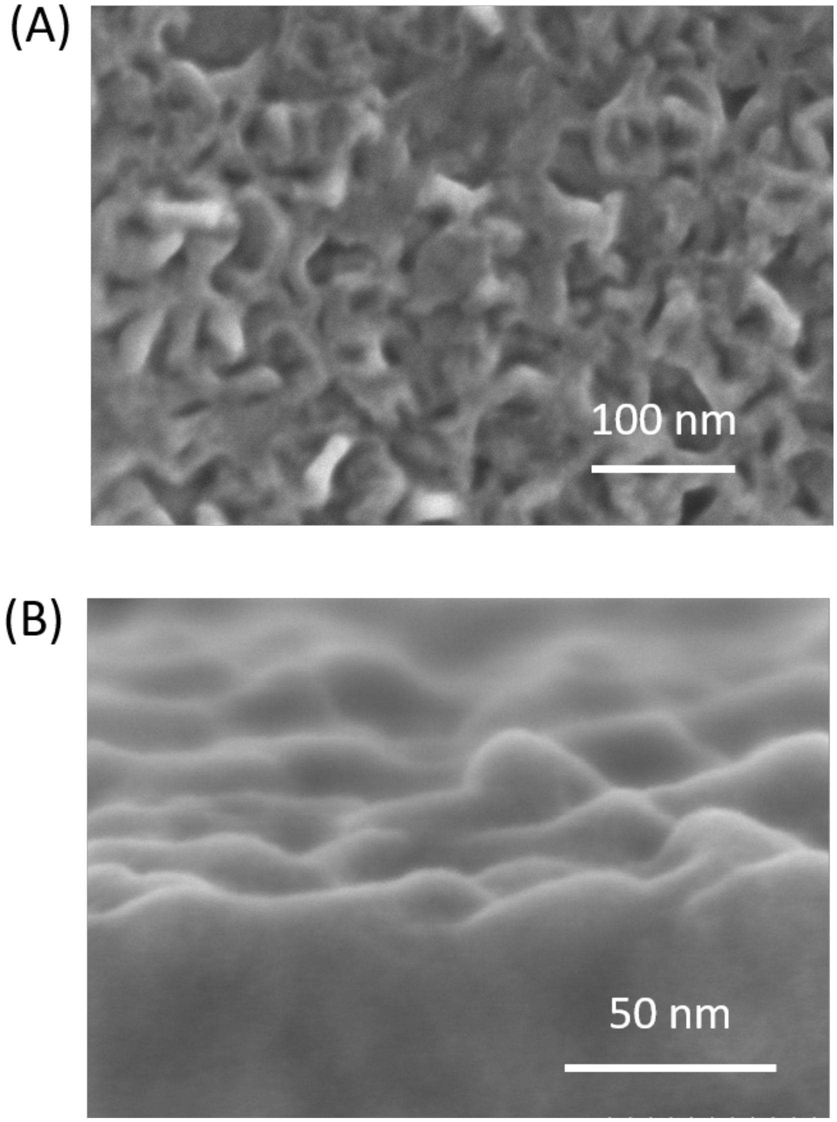

Fig. S5 (A) A top-view and (B) a cross sectional SEM images of TiN-f.

<S6> LDI mass spectra acquired for small molecules using the TiN-p substrate.

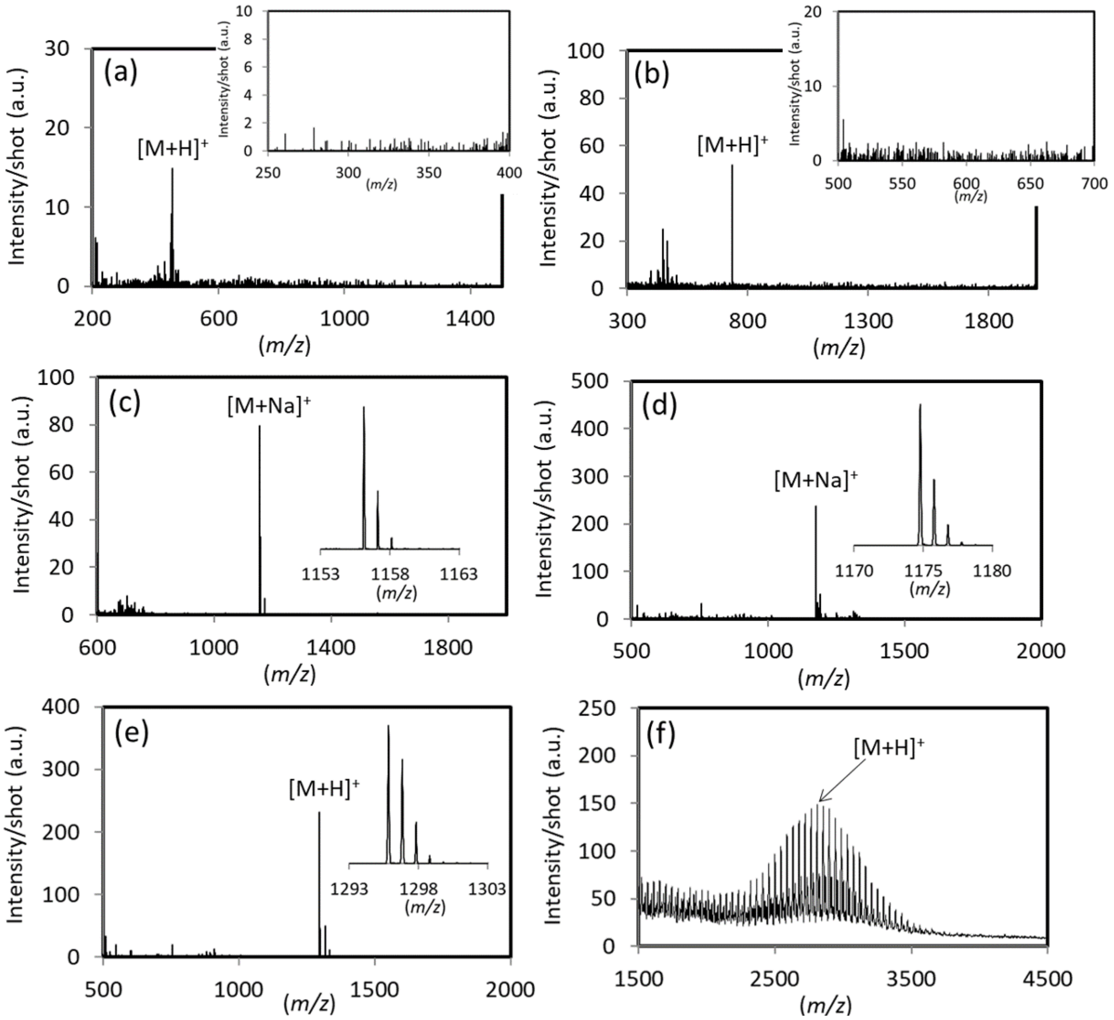

Fig. S6 Averaged mass spectra of (a) verapamil (1.0 pmol/μL), (b) DpPC (5.0 pmol/μL), (c) β-CD (2.5 pmol/μL), (d) maltoheptaose (5.0 pmol/μL), (e) A1 (1.0 pmol/μL), and (f) PEG4000 (2.5 pmol/μL) obtained using the TiN-p substrate. The insets in (a, b) are enlarged images of the *m/z* region where typical fragment ions are detected. The insets of (c, d, and e) display isotopic distributions. Peaks corresponding to sodium ion adducts $[M+Na]^+$ were observed for β-CD and maltoheptaose, accompanied by their well-resolved isotopic distribution patterns (c, d). During the detection of sugars, alkali cation adducts are likely to be detected rather than protonated adducts because these materials have high affinities for alkali metals.

<S7> LDI mass spectra acquired using the TiN-f substrate.

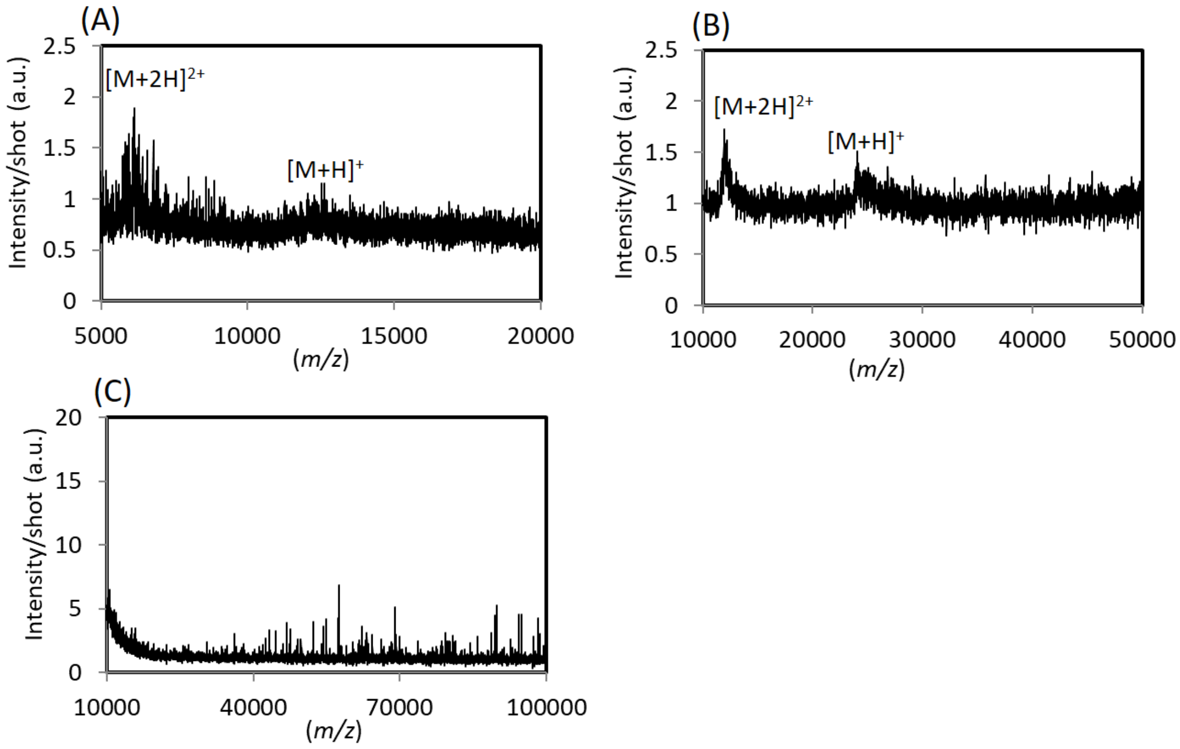

Fig. S7 Averaged mass spectra of (A) cytochrome c (5.0 pmol/μL), (B) trypsinogen (5.0 pmol/μL), and (C) BSA (5.0 pmol/μL) obtained using the TiN-f substrate. The spectra were collected in the identical conditions as that used for TiN-p.

<S8> TiN nanoparticle assisted LDI-MS for A1.

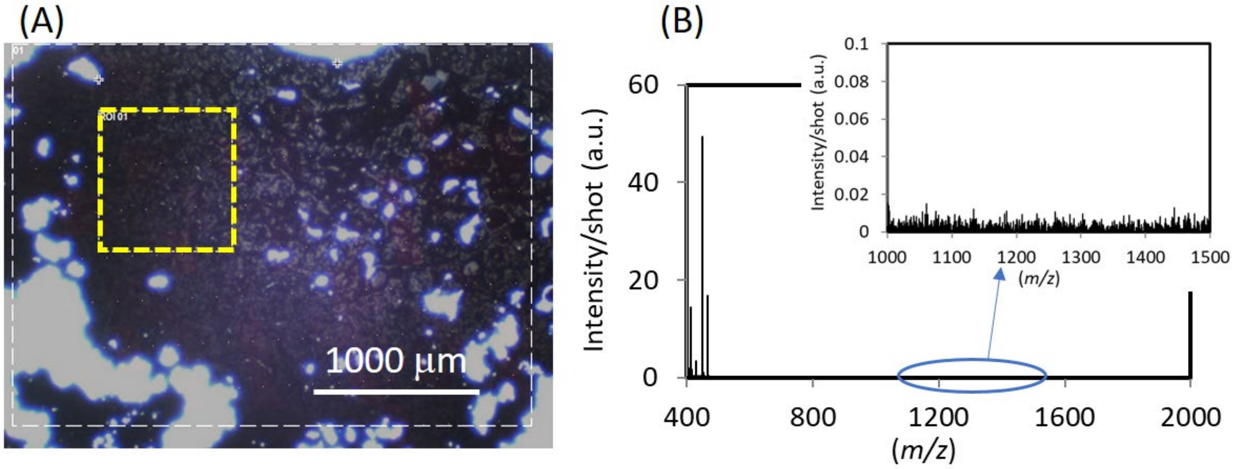

Fig. S8 LDI of A1 using TiN nanoparticles as an analytical substrate. (A) An optical image of TiN nanoparticles deposited on the Si substrate. The analytical spot where TiN nanoparticles seem to be densely packed is outlined in yellow dotted line. (B) An averaged mass spectrum generated from the yellow dotted area in (A). The inset in (B) is a magnified image, indicating no signal detection of A1. The simple "dried-droplet" method is applied on the surface of TiN-f, which only leads to propagate the droplet throughout the grains.

<S9> Contact angle of water on the TiN-p substrate.

CA: 101±0.1°

Fig. S9 A static contact angle image of water droplet on the surface of the TiN-p substrate. A 0.5 μL droplet of water was deposited onto the surface of the TiN-p substrate using a DM-501 (Kyowa Interface Science Co., Ltd.). The average value was determined by five measurements on different areas of a sample.

<S10> MALDI-MS spectra of trypsinogen.

Fig. S10 shows MS images and the signal-intensity distributions for MALDI-MSI of trypsinogen. Signals were detectable over the whole sample for 5.0 pmol/μL, whereas analyte molecules were only detectable at the periphery of the sample area for 0.5 pmol/μL (Figs. S10a and S10b). The phenomenon is in good agreement with the sweet spots generated at the rim of the sample spot when the dried droplet method was used. In MALDI-MS, oligomeric ions ($[2M+H]^+$ and $[3M+H]^+$) were observed in addition to the mono protonated ion $[M+H]^+$; such signals derived from oligomeric ions were not observed by TiN-p-MS (Fig. 4f). The presence of signals for oligomeric ions indicates protein aggregation during conventional matrix preparation. It should be noted that conventional MALDI-MSI uses various sample-preparation techniques, such as two-layer,[7] crushed crystal,[8] and fast solvent evaporation methods [9] to greatly improve quantitativity and shot-to-shot reproducibility. However, to compare LDI performance as well as the user-friendliness of the sample preparation procedure, we used the most simple “dried-droplet” method in this study for both MALDI-MSI and TiN-p-MSI.

7. Zhang, N.; Doucette, A.; Li, L. *Anal. Chem.* **2001**, *73*, 2968–2975.
8. Xiang, F.; Beavis, R. C. *Rapid Commun. Mass Spectrom.* **1994**, *8*, 199–204.
9. Vorm, O.; Roepstorff, P.; Mann, M. *Anal. Chem.* **1994**, *66*, 3281–3287.

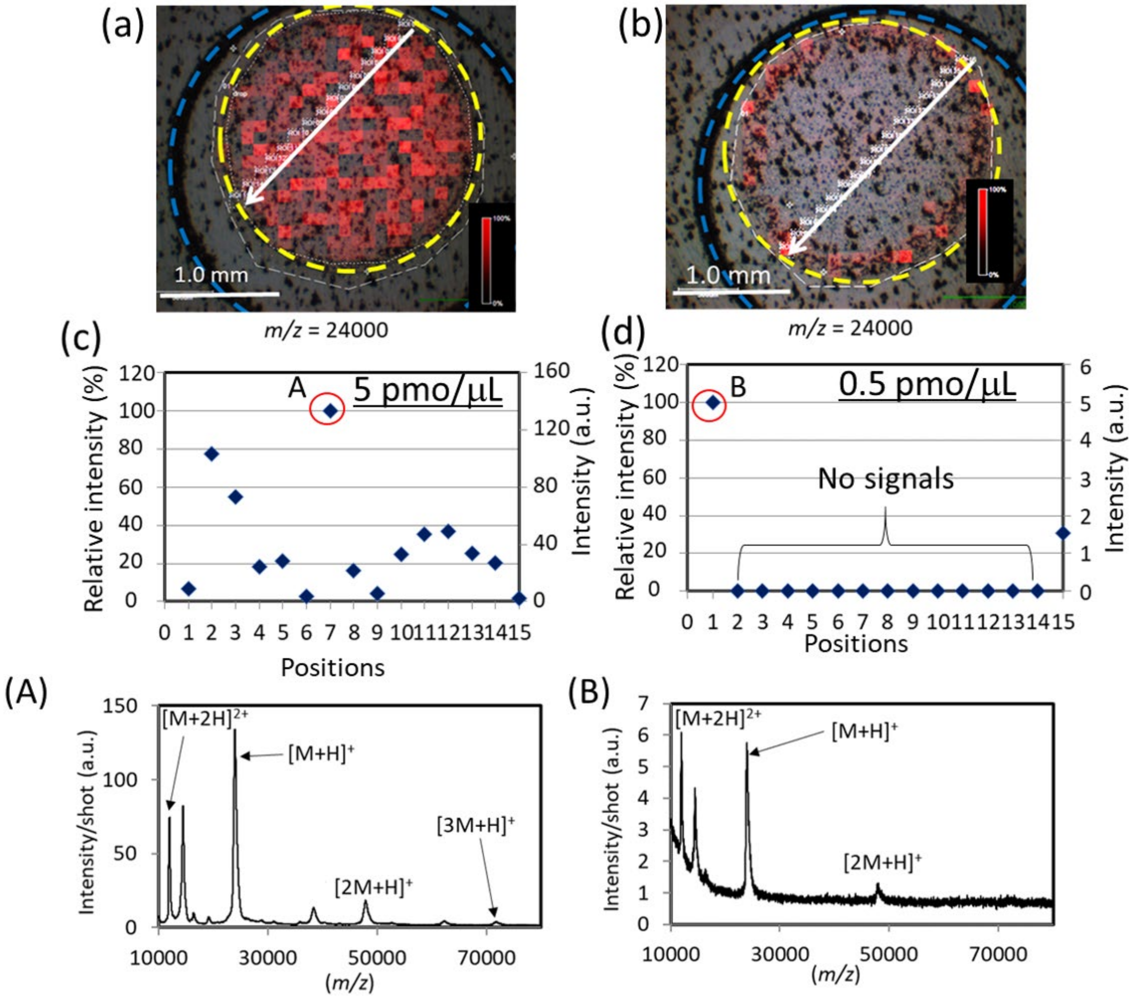

Fig. S10 MALDI-MSI of trypsinogen. (a, b) MS ion images. The droplet boundaries are indicated by yellow dotted lines, while the blue dotted lines show spot rims on the MALDI target plate in panels. (c, d) Variations in the relative signal intensities of trypsinogen (left axes) and signal intensity (right axes) obtained from the MS ion images in the same column. The data were collected from different sample spots along the white arrows shown in the corresponding MS image, where the highest signal intensity was set to 100%. Numbers on the horizontal axes correspond to measurement points along the white arrows, from the starting point to the terminal, as depicted in the MS images. A S/N ratio > 3 was used as the signal detection criterion. The concentrations of trypsinogen were: (a, c) 5.0 pmol/μL, and (b, d) 0.5 pmol/μL. (A, B) The representative MS spectra obtained from the point depicted in (c) and (d), respectively.

<S11> Log-log plots of the signal intensities of adenosine prepared in human plasma with different concentrations using the TiN-p substrate.

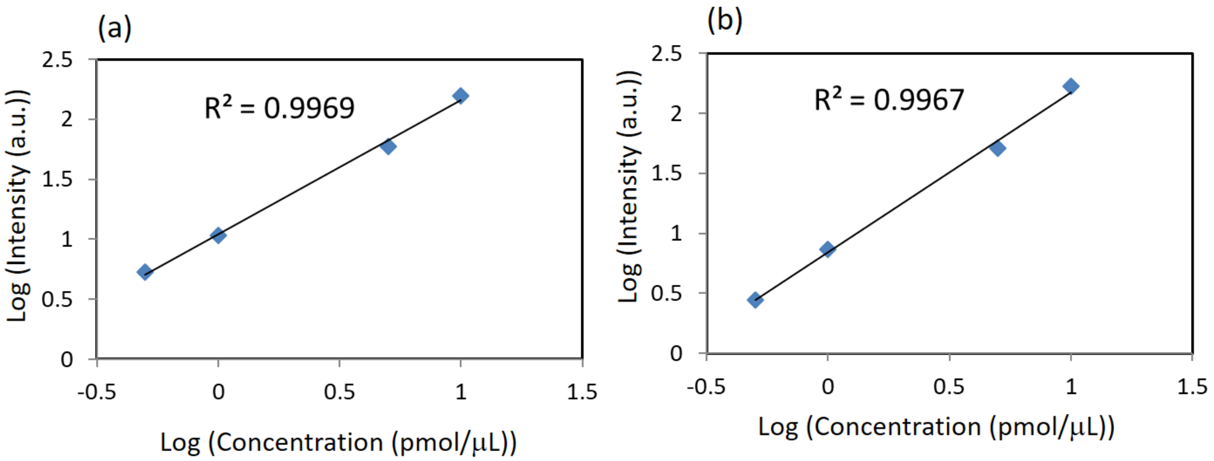

Fig. S11 Log-log plots of the signal intensities of adenosine with different concentration obtained using the TiN-p substrate. Mass spectra were collected using adenosine at concentrations ranging between 0.5 – 10.0 pmol/µL. The data were acquired without (a) and with (b) human blood plasma. The coefficient of determination (R^2) is shown in the graph.

<S12> LDI mass spectra acquired for mixed analytes using the TiN-p substrate.

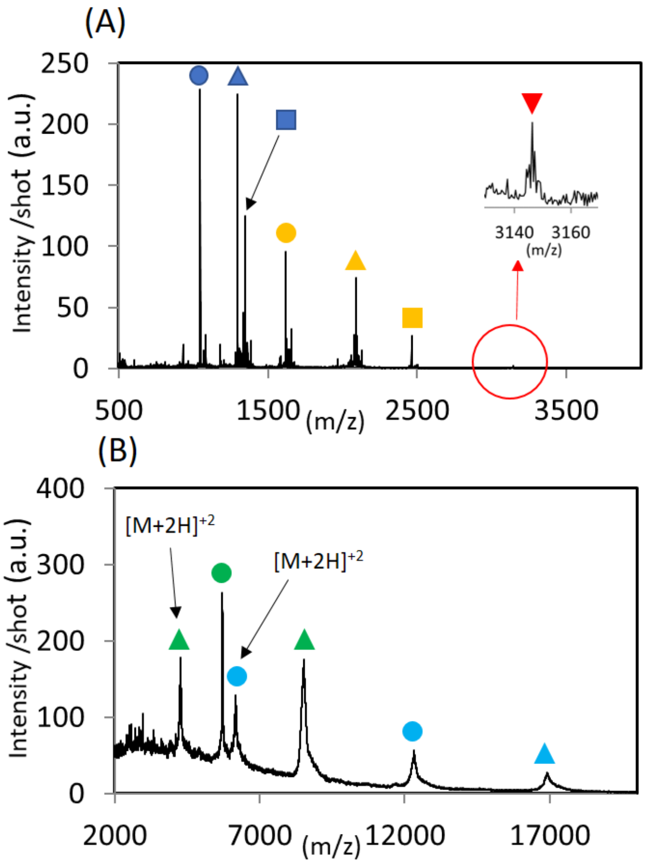

	Peptide	*m/z*	S/N
●	Angiotensin II	1045.265	477
▲	Angiotensin I	1295.178	436
■	Substance P	1347.185	220
●	Bombesin	1619.032	222
▲	ACTH clip 1-17	2091.893	196
■	ACTH clip 18-39	2463.679	51
▼	Somatostatin 28	3146.351	10

	Peptide	*[M+H]⁺ m/z*	S/N
●	Insulin	5717.578	39
▲	Ubiquitin	8534.796	37
●	Cytochrom C	12314.733	23
▲	Myoglobin	16920.547	32

Fig. S12 MS spectra of (A) peptide calibration standard and (B) protein calibration standard using TiN-p. The detected *m/z* and S/N values for each analyte molecule are tabulated beside the graph. Definition of each symbols in the graphs is listed in the tables. Both analytes were dissolved in mixtures of ACN and 0.1 vol% TFA (3/7, v/v) and 1.0 µL of the obtained solution (2.0 µM) was dropped on the TiN-p substrate. MS spectra were collected using reflectron positive-ion mode. Although the detected signal intensity gradually decreases with increasing molecular weight, all the species are detectable. $[M+2H]^{2+}$ ions were also observed for ubiquitin and cytochrome c in (B).

<S13> Salt tolerance of the TiN-p substrate

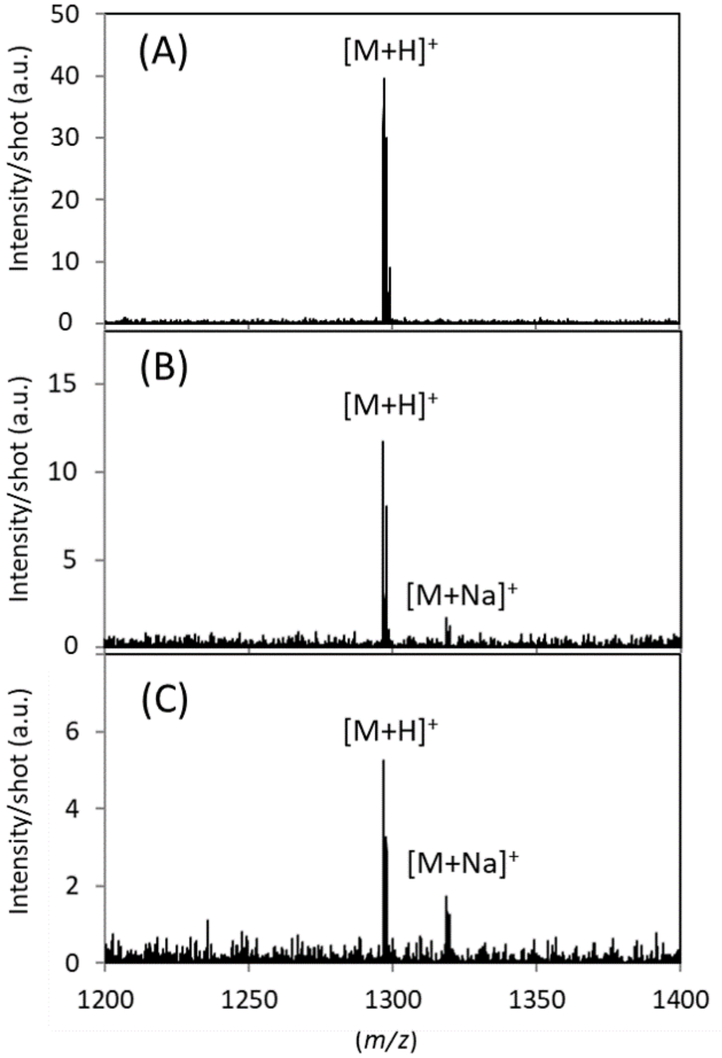

Fig. S13 Effect of salt concentration on the mass spectra of A1 (0.5 pmol/μL). (A) 0, (B) 0.5, and (C) 1 mM of NaCl was dissolved in a mixture of ACN and 0.1 vol% TFA (3/7, v/v). 1 μL of the sample solution with NaCl was applied on the surface of the TiN-p substrate. With increasing the salt concentration, the signal intensity of the protonated ion gradually decreased, and the sodium adduct ion increased.

<S14> Changes of the TiN-p substrate upon laser irradiation

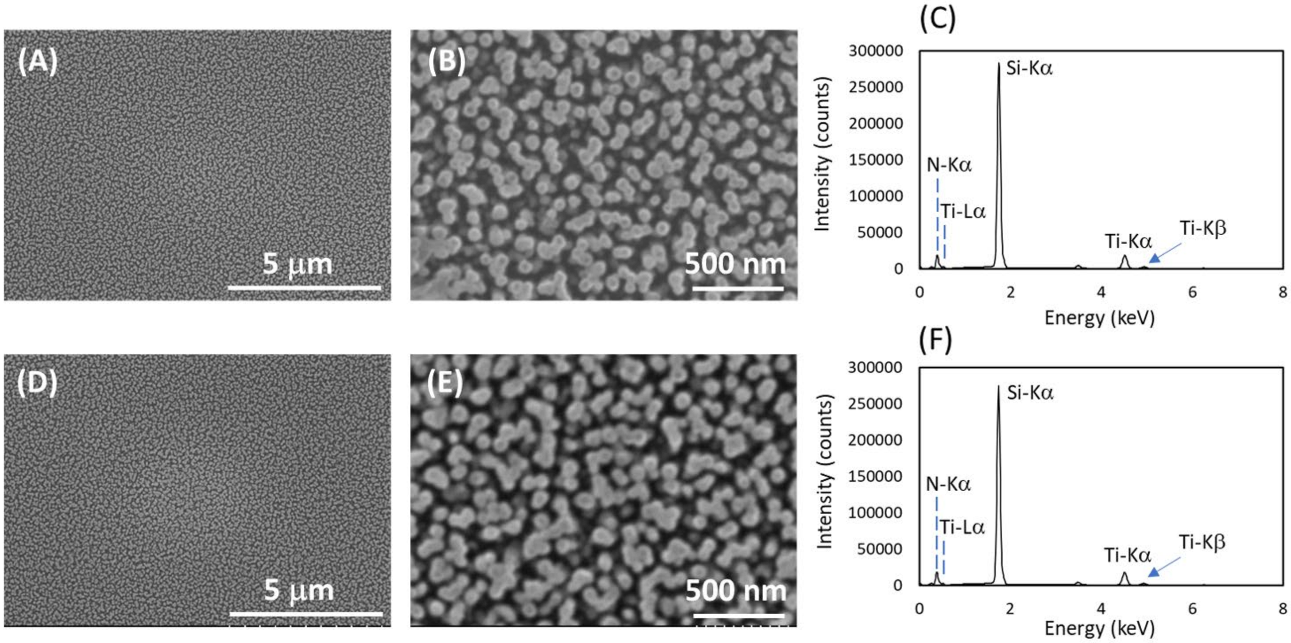

Fig. S14 SEM and Energy Dispersive X-ray Spectroscopy (EDS) analysis of the TiN-p substrate before (A, B, C) and after (D, E, F) laser irradiation with a laser power of 50% (the measurement condition for Fig. S6). The analysis was performed on a Hitachi SU-5500 (Tokyo, Japan). No change was observed for the TiN-p substrate morphologically and compositionally upon laser irradiation.

<S15> Electromagnetic field simulation details.

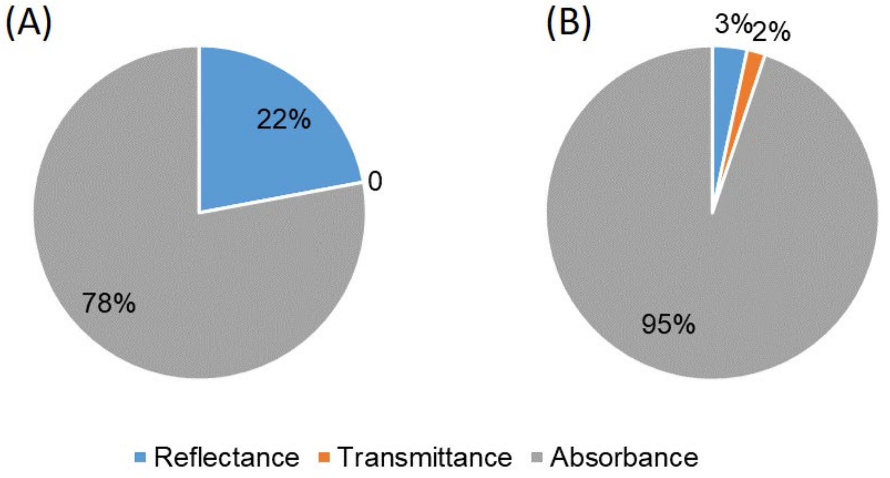

Fig. S15 Ratio of the reflectance, transmittance, and absorbance of the electromagnetic wave at 355 nm for (A) TiN film and (B) TiN pillars.

<S16> Heat-flow simulation of Si pillars.

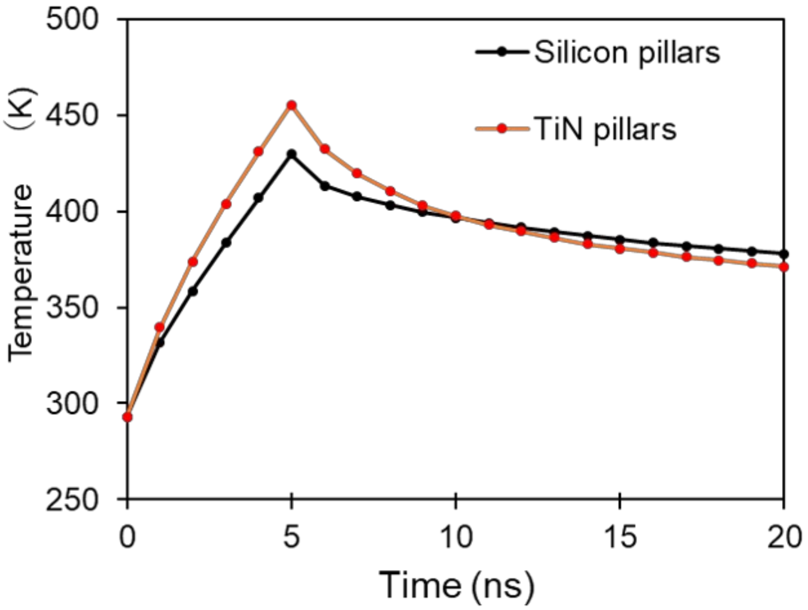

Fig. S16 Comparison of the temperature change as a function of time after the irradiation of the electromagnetic wave (355 nm) obtained for TiN pillars and Si pillars.